Self-Assembly of Disk-Shaped Molecules to Coiled-Coil Aggregates with Tunable Helicity

H. Engelkamp, S. Middelbeek, R. J. M. Nolte*

A disk-shaped molecule with chiral tails is shown to form long fibers of molecular diameter and micrometer length by self-assembly in chloroform. The molecules are derived from crown ethers and contain a phthalocyanine ring. In the fibers, they have a clockwise, staggered orientation that leads to an overall right-handed helical structure. These structures, in turn, self-assemble to form coiled-coil aggregates with left-handed helicity. Addition of potassium ions to the fibers leaves their structure intact but blocks the transfer of the chirality from the tails to the cores, leading to loss of the helicity of the fibers. These tunable chiral materials have potential in optoelectronic applications and as components in sensor devices.

Helical architectures are very common in nature. The best studied examples are the double helices formed by DNA and the α-helical motives in proteins. These biopolymers adopt helical conformations spontaneously, because of the molecular information present in their building blocks. In many cases they assemble further to form superstructures that are also helical, but often have opposite handedness. Collagen, for example, is composed of three left-handed helices, which wind around each other to give a right-handed supercoil (*1*). The so-called heavy chains of myosin self-assemble to generate extended α-helical coiled coils composed of six polypeptide chains that have a rodlike structure with an overall length of more than 100 nm (*2*). Another archetypal helical structure based on self-assembly is the tobacco mosaic virus. The individual protein molecules of this virus spontaneously form a right-handed helix when mixed with the viral DNA molecule (*3*).

One of the goals of chemistry is to achieve control over the structure of synthetic molecules and macromolecules, opening the way for new applications, for example, in the fields of catalysis and electronics (*4*). A great variety of interactions can be exploited, such as hydrogen bonding, van der Waals interactions, π-π stacking, and electrostatic interactions. Recent studies have reported the formation of superstructures driven by π-π–stacking interactions (*5*), for example, the helical folding of polymers and the formation of helical lyotropic phases. We present here an unusual example of helix and superhelix formation based on the self-assembly of disk-shaped molecules driven by π-π–stacking interactions. The helicity in these superstructures is controlled by chiral centers remote from the sites of interaction and can be tuned by the addition of K^+ ions.

The molecule (**1**) that forms the superhelix (Fig. 1) contains a phthalocyanine ring to which four benzo crown ether moieties are attached. The peripheral aromatic rings of the molecule are each di-substituted with chiral alkoxy tails. The overall diameter of the disk with extended tails is 60 Å and its thickness is 3.4 Å. The phthalocyanine core in **1** has an extended system of π-electrons. Such π-systems are responsible for the observed conductivity of electrons and excitons in stacked phthalocyanines (*6*). The crown ether moieties have potential as ion conductors (*7*), and the chiral tails can induce liquid-crystalline behavior (*8*).

The preparation of **1** will be described in detail elsewhere (*9*). It involves a straightforward 10-step synthesis (Scheme 1). When **1** is heated in an organic solvent, for example chloroform, at concentrations >5 mg/ml, and then cooled slowly, strong aggregation of the molecules to an organogel takes place. Electron micrographs (Fig. 2A) show that this gel is composed of long, left-handedly twisted fibers, which have nanometer diameter and micrometer length. The bundles typically contain up to 25 fibers, each with the diameter of one single phthalocyanine molecule (60 Å).

Electronic absorption spectroscopy could in principle provide information on the type of aggregated structures that are present (*6*). However, at the very low concentrations (~10 μM) required for optical and circular dichroic (CD) spectroscopy studies on phthalocyanines, no aggregation of **1** was observed in chloroform. Aggregation could be induced by increasing the polarity of the solvent. In a mixture of chloroform and methanol (1:1 v/v), **1** was partly aggregated even at very low concentrations, as could be inferred from the blue-shifted Q-bands of the phthalocyanine rings that appeared at 600 nm (Fig. 3A, top). In nonaggregated **1**, they are located at 630 and 700 nm. This shift is caused by exciton coupling between neighboring phthalocyanines in a stack (*6*). A couplet (bisignate signal) was present in the CD spectrum at the same wavelength. The sign of this couplet (Fig. 3A, bottom) suggests the presence of a right-handed helical arrangement of the transition dipoles of the phthalocya-

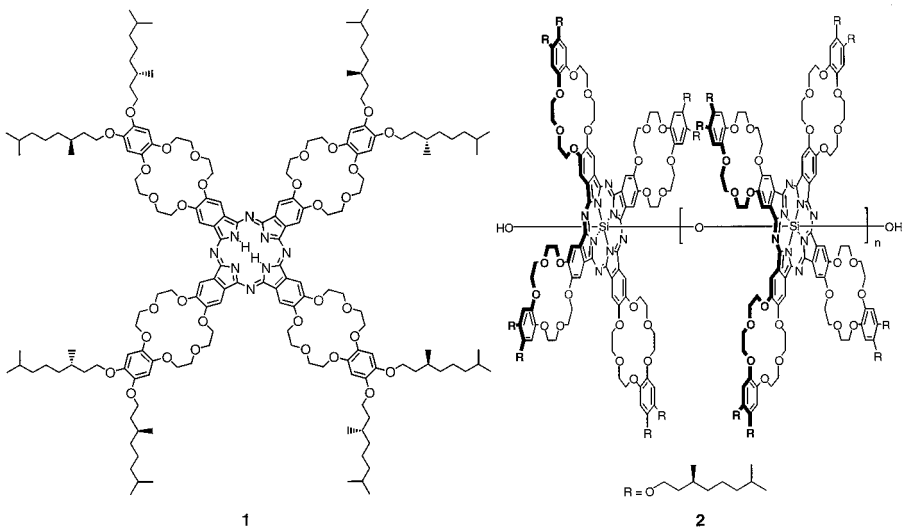

Fig. 1. Chemical structures of crown ether phthalocyanine **1** and (crown ether phthalocyaninato) polysiloxane **2**.

Department of Organic Chemistry, NSR Center, University of Nijmegen, Toernooiveld, 6525 ED Nijmegen, Netherlands.

*To whom correspondence should be addressed. E-mail: tijdink@sci.kun.nl

nines within a stack of phthalocyanine molecules in an aggregate (*10*). Three types of helicity can be imagined (Fig. 3B). First, the crown ether phthalocyanine rings may be arranged in a "spiral staircase–like" manner. Second, the rings may be positioned on top of each other, but with a staggering angle between neighboring phthalocyanines that is nearly constant and always in the same direction. Third, the normal of the plane of each phthalocyanine ring may be tilted and gradually rotated along the stacking axis. In order to differentiate between these structures, we synthesized the dihydroxy-phthalocyaninatosilicon derivative of **1**, which was polymerized to give phthalocyaninato-polysiloxane **2** (*11*) (Fig. 1). Polymer **2** has a polysiloxane backbone, to which the crown ether phthalocyanine units are attached in a skewered fashion, giving a shish kebab–like structure. The CD spectrum of the covalent polymer in chloroform shows the same couplet in the Q-band region (Fig. 3A, bottom, blue line) as the self-assembled noncovalent polymer (Fig. 3A, bottom, red line), again indicative of a right-handed helical structure. For steric reasons, the only possible helical structure for the polysiloxane polymer is type 2 in Fig. 3B (*12*). X-ray powder diffraction revealed that in the noncovalent stack of **1**, the phthalocyanine cores are at a distance of 3.4 Å, which would be very short if structures of type 1 or 3 had been formed. These combined results suggest that the arrangement of the molecules within the self-assembled stack, as well as in the classical polymer, is most likely that of type 2 in Fig. 3B.

Scheme 1. Synthesis of crown ether phthalocyanine **1**. (i) Br_2, CH_2Cl_2, 0°C (80%); (ii) chloroethoxyethanol, NaI, Na_2CO_3, acetonitrile, 80°C (61%); (iii) *p*-toluenesulfonyl chloride (Tos = *p*-toluenesulfonyl), pyridine, −10°C (80%); (iv) 3,4-dihydroxybenzaldehyde, K_2CO_3, *N*,*N*-dimethylformamide (DMF), 120°C (59%); (v) H_2O_2, H_2SO_4, methanol, 20°C (65%); (vi) $(KSO_3)_2NO$, *N*(*n*-butyl)$_4$Cl, KH_2PO_4, H_2O, tetrahydrofuran, room temperature (98%); (vii) Zn, acetic acid, acetic anhydride, 80°C (80%); (viii) (*S*)-3,7-dimethyloctyl bromide, NaOH, *n*-butanol, 118°C (59%); (ix) CuCN, pyridine, DMF, 153°C (60%); and (x) *N*,*N*-dimethylaminoethanol, 135°C (20%).

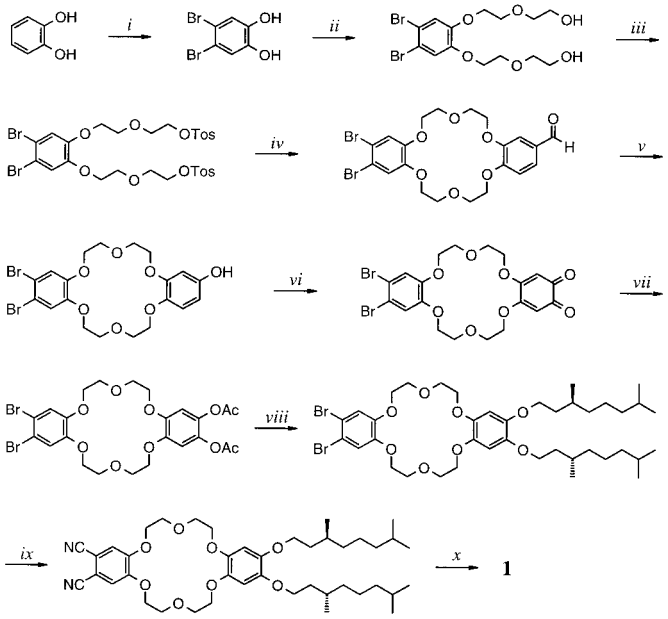

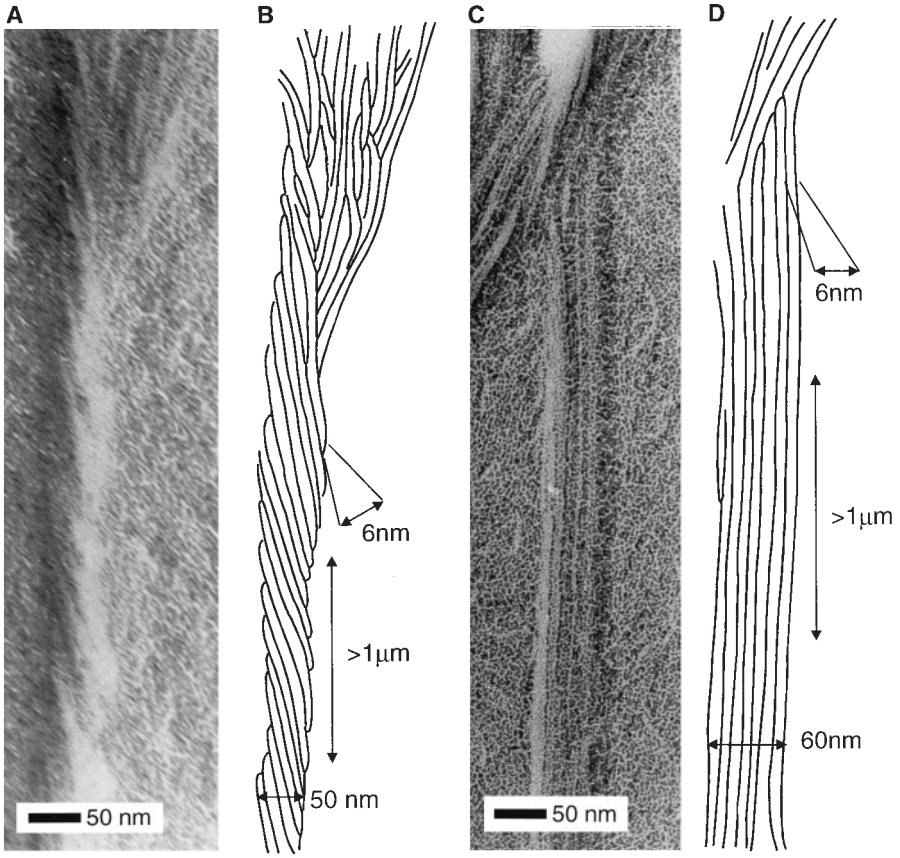

Fig. 2. Transmission electron micrographs (platinum shadowing) of gels from compound **1**. (**A**) Left-handed coiled-coil aggregates in chloroform. (**B**) Schematic representation of the helices in (A). (**C**) Nonhelical rods formed in chloroform in the presence of KCl. (**D**) Schematic representation of the rods in (C).

A fiber with a right-handed twist and a type 2 structure has a "grooved" exterior. In order to maximize the van der Waals contact between two fibers twisted around each other (Fig. 3C), each of them has to bend over in order to fit into the groove of the other fiber. The tilting angle between the two fibers is called the crossing or crossover angle. This angle is double the angle of the groove with respect to the stacking axis, which in turn depends on the dimensions of the monomer, and the staggering angle between two monomers according to

$$\alpha = 2 \arctan\left(\frac{D\phi}{2d}\right) \qquad (1)$$

where α is the crossing angle, d the interplanar stacking distance, D the diameter, and ϕ the staggering angle in radians. In the case of our crown ether phthalocyanine rings, with D = 60 Å and d = 3.4 Å, we calculate using Eq. 1 that for staggering angles larger than 6.5°, the crossing angle becomes larger than 90°, and a supercoiled structure is formed that has a helical sense opposite to that of the original helix. From the crossing angle measured in the electron micrographs (125°), a staggering angle of 12° could be estimated.

The experiments described above indicate that chiral information is transferred from the (*S*)-chiral centers in the tails of **1** to the cores,

where it is amplified to give right-handed helical fibers, which then further pack into left-handed supercoils. If this analysis is correct, it should be possible to block the chirality transfer by forcing the molecular disks into an eclipsed (face to face) conformation instead of a staggered one, in which case the helical structure should be lost.

We tested this possibility by adding K^+ ions to the fibers. Crown ethers form stable complexes with alkaline metal ions (*13*). In order to investigate what type of complexes are formed between compound **1** and K^+ ions, a titration experiment was performed in chloroform. Unsubstituted 18-crown-6 forms solely 1:1 complexes with K^+ ions. The Q-band regions of the electronic absorption spectra of a dilute solution of compound **1** in chloroform with different amounts of potassium picrate (Fig. 4A, left) show that the spectrum of pure **1** and the spectrum of **1** saturated with K^+ ions are nearly identical (red lines), whereas the spectrum of **1** with approximately two equivalents of K^+ (dark blue line) is rather different. The latter spectrum is that of a mixture of cofacial phthalocyanine dimers (characteristic absorption at 630 nm) and nonaggregated phthalocyanines. The direct conversion of these two species follows from the intersection points (isosbestic points) in the series of spectra (Fig. 4A, right) (*14*). The largest difference in the spectra occurs at 700 nm, where the Q-band of nonaggregated phthalocyanine is located. These results suggest that at low concentrations, K^+ ions are shared between two crown ether units of two different phthalocyanines. In this way, four ions can be accommodated by two crown ether phthalocyanine rings, similar to the way lawn bowling balls are held in a container (Fig 4B). This process will be facilitated because attractive π-π interactions occur between the aromatic rings. When more than two equivalents of potassium picrate are added, the crown ethers start to take up one K^+ ion in each ring, which leads to separation of the sandwichlike complexes. We found that the dimer complex did not show any CD activity, suggesting that the crown ether phthalocyanines within it have an eclipsed conformation.

A solution of **1** in chloroform was heated in the presence of solid KCL, filtered, and then cooled, which again resulted in the formation of an organogel. Electron micrographs of this gel show that almost no helical structures are present (Fig. 2C). The fibers look remarkably similar to those formed by an achiral liquid crystalline crown ether phthalocyanine (*15*). The disappearance of helicity can be explained by assuming that the metal ions are located dynamically in, or between, the crown ether rings. In this way, the transfer of chirality is blocked because the phthalocyanines are forced to adopt an eclipsed conformation, as outlined above.

The results presented here provide insight into how chiral information can be trans-

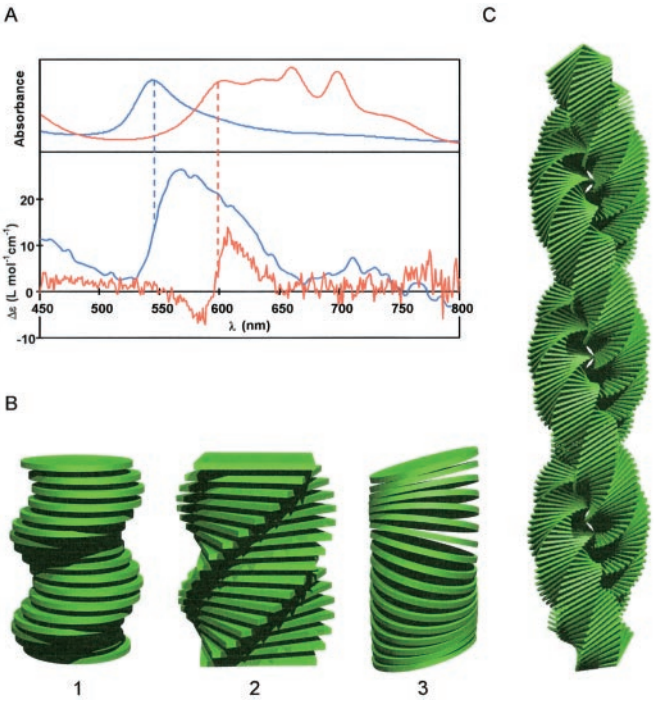

Fig. 3. (**A**) Electronic absorption spectra in arbitrary units (top) and CD spectra (bottom) of **1** (red line) and polymer **2** (blue line). (**B**) Three types of helical aggregates that may be formed by **1**. The molecules are represented as disks in 1 and 3 and as squares in 2 to show more clearly the helical packing arrangement of the building blocks. (**C**) Calculated model (*16*) of a coiled-coil from **1** reproducing the observed handedness of the single fibers and the superstructure. For the calculation the following parameters (Eq. 1) were used: ϕ = 12°, d = 3.4 Å, D = 60 Å.

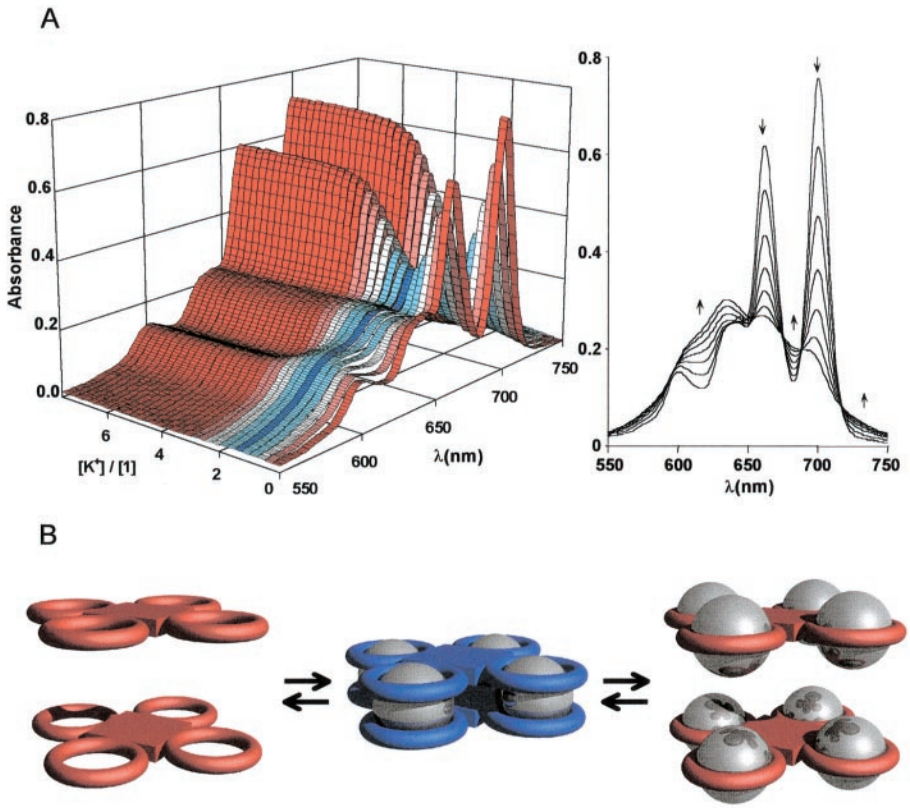

Fig. 4. (**A**) (Left) Electronic absorption spectra of **1** in chloroform (concentration 10 μM) as a function of the ratio of potassium picrate and **1**. (Right) Isosbestic points at 597, 650, 675, 688, and 717 nm that appear when the $[K^+]/[\mathbf{1}]$ ratio is increased from 0 to 2. The arrows indicate increasing potassium picrate concentration. (**B**) Schematic representation of the formation and breakdown of the sandwich-type complexes between K^+ ions and **1**.

ferred and expressed in synthetic systems in a way similar to nature. An interesting mechanism is suggested by which chirality is amplified to give supramolecular (helical) chirality, namely through the following processes: The S-chiral centers in the tails induce a clockwise orientation of the molecular disks which, aided by strong π-π stacking, leads to the formation of fibers with right-handed helicity. Side-on aggregation of the fibers subsequently yields supercoiled structures with left-handed helicity. Such a control over chirality may be valuable in designing new materials for optoelectronic applications. The present chiral fibers are attractive candidates for use as nonlinear optical materials and as components in sensor devices, for example, for the detection of alkali metal ions.

References and Notes

1. D. R. Eyre, *Science* **207**, 1315 (1980).
2. A. D. McLachlan, *Annu. Rev. Biophys. Bioeng.* **13**, 167 (1984).
3. R. E. Franklin, *Nature* **175**, 379 (1955); _____ and A. Klug, *Acta Crystallogr.* **8**, 777 (1955).
4. D. Goldhaber-Gordon *et al.*, *Proc. IEEE* **85**, 521 (1997).
5. R. S. Lokey and B. L. Iverson, *Nature* **375**, 303 (1995); J. C. Nelson *et al.*, *Science* **277**, 1793 (1997); G. S. Hanan *et al.*, *J. Chem. Soc. Chem. Commun.* (1995), p. 765; D. M. Bassani *et al.*, *Angew. Chem. Int. Ed. Engl.* **36**, 1845 (1997); P. Mariani, F. Ciuchi, L. Saturni, *Biophys. J.* **74**, 430 (1998); N. Kimizuka *et al.*, *J. Chem. Soc. Chem. Commun.*, 2103 (1995).
6. C. C. Leznoff and A. B. P. Lever, Eds., *Phthalocyanines, Properties and Applications* (VCH, New York, 1989–1996), vols. 1 to 4.
7. T. M. Fyles and W. F. van Straaten-Nijenhuis, in *Comprehensive Supramolecular Chemistry*, J. L. Atwood, *et al.*, Eds. (Elsevier Science, Oxford, 1996), vol. 10, chap. 3.
8. J. F. van der Pol *et al.*, *Liq. Cryst.* **6**, 577 (1989).
9. H. Engelkamp, S. Middelbeek, R. J. M. Nolte, in preparation.
10. N. Harada and K. Nakanishi, *Circular Dichroic Spectroscopy—Exciton Coupling in Organic Chemistry* (Oxford Univ. Press, Oxford, 1983), pp. 6–9.
11. W. Caseri, T. Sauer, G. Wegner, *Makromol. Chem. Rapid Commun.* **9**, 651 (1988).
12. H. Engelkamp, C. F. van Nostrum, S. J. Picken, R. J. M. Nolte, *Chem. Commun.*, 979 (1998).
13. C. J. Pedersen, *J. Am. Chem. Soc.* **89**, 7017 (1967).
14. O. E. Sielcken *et al.*, *ibid.* **109**, 4261 (1987).
15. C. F. van Nostrum *et al.*, *ibid.* **117**, 9957 (1995).
16. Persistence of Vision(tm) Ray-Tracer [POV-Ray(tm)] version 3.02, Persistence of Vision Development Team (tm).

17. Funded by the Netherlands Foundation for Chemical Research with financial aid from the Netherlands Organization for Scientific Research.

6 January 1999; accepted 22 March 1999

Pressure-Induced Solid Carbonates from Molecular CO_2 by Computer Simulation

S. Serra,[1,2] C. Cavazzoni,[1,2] G. L. Chiarotti,[1,2]* S. Scandolo,[1,2] E. Tosatti[1,2,3]

A combination of ab initio molecular dynamic simulations and fully relaxed total energy calculations is used to predict that molecular CO_2 should transform to nonmolecular carbonate phases based on CO_4 tetrahedra at pressures in the range of 35 to 60 gigapascals. The simulation suggests a variety of competing phases, with a more facile transformation of the molecular phase at high temperatures. Thermodynamically, the most stable carbonate phase at high pressure is predicted to be isostructural to SiO_2 α-quartz (low quartz). A class of carbonates, involving special arrangements of CO_4 tetrahedra, is found to be more stable than all the other silica-like polymorphs.

Carbon and silicon, although isoelectronic and close in their solid state behavior in several ways, differ markedly when fully oxidized. In carbon, the stability of CO_2 is so overwhelming that no other nonmolecular solid state forms are known. In silicon, by contrast, the phase diagram is dominated by solid state silicates, because the stability of molecular SiO_2 is poorer than that of CO_2. The wide range of electrical and optical applications of SiO_2 quartz (such as piezoelectricity and optical nonlinearities) derive from its noncentrosymmetric crystal structure. If CO_2 could be synthesized in a covalently bonded noncentrosymmetric structure, these properties would be complemented by the higher mechanical strength of the less deformable C–O covalent bond with respect to the Si–O one. Here we present theoretical calculations and simulations, indicating that ultrahigh pressures should reduce the stability of molecular CO_2 in favor of quartzlike nonmolecular solid state carbonates.

The crystalline structure of solid molecular CO_2 is characterized by the large quadrupole moment of the linear CO_2 molecule, which dominates the long-range intermolecular interactions (*1, 2*). The cubic Pa3 structure (α-CO_2) prevails at room temperature for pressures lower than 11 GPa (*3–5*). With increasing pressure above 11 GPa, a second quadrupolar molecular phase, an orthorhombic *Cmca* (β-CO_2) (Fig. 1A), prevails (*5, 6*). This *Cmca* molecular phase persists to at least 50 GPa (*7, 8*), but no further knowledge is presently available of additional phase transition, before eventual pressure-induced chemical decomposition (*9*).

We have explored this unknown pressure region by constant pressure molecular dynamics (MD) simulations based on the variable-cell method (*10*). The first-principles density functional nature of the method and the variable cell dynamics are effective for simulating pressure-induced solid-solid phase transformations in a variety of systems (*11*), including the characterization of the pressure-induced polymerization of carbon monoxide (*12*). The density functional scheme used is based on the Becke-Lee-Yang-Parr generalized gradient-corrected local density approximation (LDA/GGA) (*13*), and nonlocal (*14*) pseudopotentials for ion cores (*15*). Wavefunctions for MD simulations were expanded in plane waves with an energy cutoff of 80 Ry and Γ point sampling of the Brillouin zone (BZ). Final electronic and structural refinements were obtained by fully converged k-point sampled calculations and 100 Ry cutoff.

The validity of the computational scheme was initially checked by comparing our optimized β-CO_2 molecular lattice structure with the x-ray data at 12 GPa (*5*). Our calculated structures are consistent with the experimentally derived structure, especially in the fully converged k-points calculations [256 k-points in the full BZ], where errors in the lattice constants are less than 0.3%. Moreover, the tilt angle of the molecules relative to the *c* axis, usually difficult to reproduce because of its weak energy dependence, is calculated to be 52.5°, consistent with the experimental value of 52°. We also confirm, as already found by Gygi (*6*), that molecules lie in the plane identified by the *c* axis and the shorter axis of the basal plane. These results show that the LDA/GGA description of solid molecular CO_2 can be used to explore the high-pressure phase diagram of solid CO_2.

The first MD simulation was started with an orthorhombic simulation box containing 16 CO_2 molecules initially in the β-CO_2 phase at 12 GPa, with a time step of 0.3 fs. The temperature was equilibrated (*16*) at 300 K for 3 ps, during which the β-CO_2 structure remained stable. Pressure was then increased

[1]International School for Advanced Studies (SISSA), Via Beirut 4, I-34014 Trieste, Italy. [2]Istituto Nazionale per la Fisica della Materia (INFM), Via Beirut 4, I-34014 Trieste, Italy. [3]International Center for Theoretical Physics (ICTP), Post Office Box 586, I-34014 Trieste, Italy.

*To whom correspondence should be addressed. E-mail: guido@sissa.it